Rheol Acta (2006) 45: 435–443
DOI 10.1007/s00397-005-0067-x

ORIGINAL CONTRIBUTION

Pierre Terech
Séverine Friol
Neralagatta Sangeetha
Yeshayahu Talmon
Uday Maitra

Self-assembled nanoribbons and nanotubes in water: energetic vs entropic networks

Received: 24 June 2005
Accepted: 2 November 2005
Published online: 13 December 2005

Paper presented at the Annual Meeting of the European Society of Rheology, Grenoble, April 2005

P. Terech (✉) · S. Friol
UMR 5819 (CEA-CNRS-Université Joseph Fourier), CEA-Grenoble, DRFMC,
17 rue des Martyrs,
38054 Grenoble Cedex 09, France
e-mail: pierre.terech@cea.fr
Tel.: +33-438-785998
Fax: +33-438-785691

N. Sangeetha · U. Maitra
Department of Organic Chemistry,
Indian Institute of Science,
Bangalore 560 012, India

Y. Talmon
Department of Chemical Engineering,
Technion-Israel Institute of Technology,
Haifa 32000, Israel

Abstract We present a comparative investigation of two opposite classes of self-assembled fibrillar networks. Ribbons and tubes having cross-sectional dimensions in the nanoscale can be formed in aqueous solutions of steroids derived, respectively, from deoxycholic (DC) and lithocholic (LC) acids. Rheological features distinguish energetic networks of DC ribbons rigidly fixed in cylindrical bundles and entropic transient networks of LC tubes weakly interacting in shear-sensitive suspensions. The two classes are characterized by their frequency sweep profiles, viscoelastic linear domains, scaling laws of the elastic shear modulus vs concentration, kinetics of formation of the networks, and their optical birefringence aspects. A theoretical context for networks of rigid fibers is used to account for the scaling exponents α in the G' (and σ^*) $\propto C^{\alpha}$ laws (α=2.0 and 1.0, respectively, for DC and LC). The evolution observed in DC gels from ribbons to cylindrical fibers with monodisperse sections made up with four ribbons is an indication of an equilibrated balance between face-to-face attractions and untwisting elastic processes of the constitutive ribbons.

Keywords Self-assembling · Networks · Fibers · Tubes · Ribbons · Rheology

Introduction

Steroid molecules are frequently used to develop supramolecular architectures operative in the gelation of liquids. The platform is versatile; various self-assembling molecules can be synthesized by coupling specific groups at the C-3 position of the steroid core. For instance, a family of thermally reversible organogels made up of aromatic (e.g., anthracene or naphthalene) grafts appended to a cholesterol moiety has been exhaustively investigated and shows a variety of straight and twisted fibers (Lin et al. 1989). Furthermore, cholesterol derivatives containing an azobenzene group have been studied for their gelating properties, revealing the existence of novel helical aggregation modes and original photoresponsive properties (Murata et al. 1994). In water, the physico-chemical properties of bile salts have been studied for a long time (O'Connor and Wallace 1985), and for instance in deoxycholate systems, different levels of aggregation have been identified in an aggregation reaction proceeding from primary (Bonincontro et al. 1999; Conte et al. 1984; Esposito et al. 1987) to secondary micelles (Mazer et al. 1979). The aggregation behavior of aqueous solutions of sodium cholate, deoxycholate, and chenodeoxycholate bile salts has also been investigated by small-angle X-ray measurements. It was shown that micelles are formed in the dilute range, whereas

an increase in concentration induces micellar size growth (Zakrzewska et al. 1990). Based on certain similarities of the X-ray scattering pattern of aqueous solutions, gel, and crystal, a common type of helical structure with an ≈21-Å diameter was proposed (Conte et al. 1984; Esposito et al. 1987). Light scattering measurements have confirmed the existence of a sphere-to-rod transition at high NaCl concentration in sodium taurodeoxycholate solutions (Schurtenberger et al. 1983). In addition, mixtures [e.g., in the presence of vaccinia virus (McCrea and Angerer 1960), glycylglycine (Rich and Blow 1958) or glycine (Campanelli et al. 1989)] with sodium deoxycholate can produce thin helical strands.

The examples illustrate the particularity of the self-assembling phenomenon for steroid derivatives. Compared to "ordinary surfactants," steroid-derived amphiphilic molecules can be described as "facial surfactants." The molecular shape has a curved and functionalized part made up of hydrophobic steroid rings bearing an intrinsic molecular chirality. We present here two types of bile salt derivatives with opposite structural, kinetic, and rheological properties in viscoelastic aqueous suspensions and gels. Not only are the structural features of the individual aggregates very different from one class to the other, their rheological behavior is also strikingly different and defines two classes of self-assembled fibrillar networks (SAFINs). The first class of steroids is made of a modified deoxycholate with a positively charged N-heterocycle graft in salted aqueous solutions (DABCO-DC). The second class is composed of the negatively charged sodium lithocholate (SLC) salt in alkaline aqueous solutions.

Material and methods

The synthesis of DABCO-DC is described elsewhere (Sangeetha et al. 2004). Lithocholic acid was from Aldrich (98% purity). DABCO-DC specimens were prepared by gentle shaking of the powder in a salted aqueous solution of sodium chloride (0.5 M). For SLC samples, the lithocholic acid was dispersed in a sodium hydroxide aqueous solution ($12<pH<13$, T_{NaOH}~0.15 M, depending on the LC concentration). Scattering experiments were performed at ILL, Grenoble, France, using the D22 low-angle spectrometer (http://www.ill.fr).

For cryo-transmission electron microscopy (cryo-TEM), we used a Philips CM120 dedicated cryo-TEM instrument, equipped with a Gatan MultiScan 791 cooled-CCD camera, and an Oxford CT-3500 cryo-holder and cryo-transfer system. Specimens were prepared at room temperature in a controlled environment vitrification system (CEVS), transferred to the TEM, and examined at about −180°C according to a well-established protocol (Talmon 1999).

Rheological measurements were carried out with an RS100 and RS600 Haake stress-controlled rheometers. A serrated plate–plate geometry (20-mm diameter, 0.6-mm gap) was applied for the DABCO-DC system. With the SLC system, appropriate cone–plate geometries were used depending on the concentration (from a serrated plate–plate 20-mm geometry to a double-cone geometry with 60-mm diameter and 1° angle). Only experiments for which an equilibrium value of the elastic shear modulus was reached have been considered for the determination of the related scaling behavior.

Optical micrographs of the gels in 1-mm quartz cells were recorded between crossed polarizers on an Olympus BX100 optical microscope at a magnification of 10×.

Results and analysis

Scheme 1 shows the chemical structure of the two steroids. DABCO-DC is a positively charged molecule derived from a 3,12-dihydroxycholane steroid. In salted (0.5 M NaCl) water, thermoreversible gels are obtained for concentrations of the order of 1 wt%. The SLC system is made up of the negatively charged sodium salt of the lithocholic bile acid. In alkaline aqueous solution (pH~12.5), viscoelastic solutions and gels are obtained depending on the concentration. The sequence of the junctions of the rings in the molecular structure is *cis-trans-trans* and accounts for the curved hydrophobic core. The chemical structure and charge of the ionized group and the number of other polarized centers (OH), potentially involved in the aggregation reaction, are molecular parameters that distinguish the DABCO-DC and SLC systems at the molecular scale (as a starting point of the investigation).

Ribbons (DABCO-DC system): energetic network

Small-angle neutron scattering (SANS) experiments can be used to identify the presence of ribbon-like morphologies in the DABCO-DC system. A previous detailed SANS study (Terech et al. 2005) has characterized the structural features of the aggregates forming the networks in the gel phases. To summarize, a sharp evolution of the scattering profile with the DABCO-DC concentration is observed.

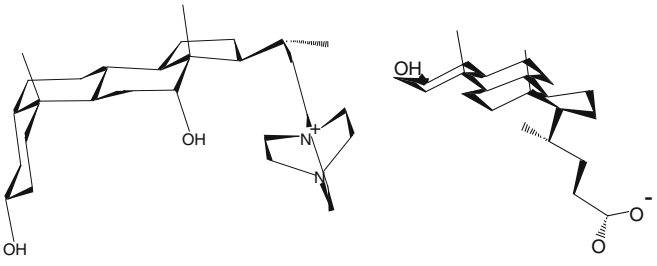

DABCO-DC **SLC**

Scheme 1 Wireframe views of DABCO-DC (left) and SLC (right) steroids

Figure 1a shows the asymptotic low-Q behaviors for cylindrical fibers ($I \propto Q^{-1}$) and lamellar-like or ribbon-like fibers ($I \propto Q^{-2}$) (Glatter and Kratky 1982). The experimental data present large-Q oscillation(s) revealing the relative monodispersity of the cross-sections. At low concentration, the transverse dimension t of the ribbons can be obtained from $\ln Q^2 I$ vs Q^2 plots appropriate for lamellar-like aggregates (Fig. 1a). The obtained value t~36.9 Å appears related to the bimolecular size. The plot also displays a low-Q plateau (Q^{-2} decay of the cross-sectional intensity) whose extension is limited in the innermost part by a sharp decrease associated to the finite spatial extension of the long side $2a$ of the cross-sections. The extracted value $2a \sim 1/\sqrt{0.0015} \sim 160$ Å indicates a moderate anisotropy of the section of fibers. The number of molecules aggregated per transverse section is extracted from the extrapolated absolute intensity at $Q \rightarrow 0$, and its value $n \sim 2$ confirms the tail-to-tail aggregation mode.

If the concentration is increased (Fig. 1c), the best agreement with the corresponding theoretical scattering profiles is obtained for cylindrical fibers (R=123 Å). The evolution from Fig. Fig. 1b,c, also summarized in Fig. 1a, suggests the existence of a secondary aggregation process involving a specific bundle formation. Interestingly, a

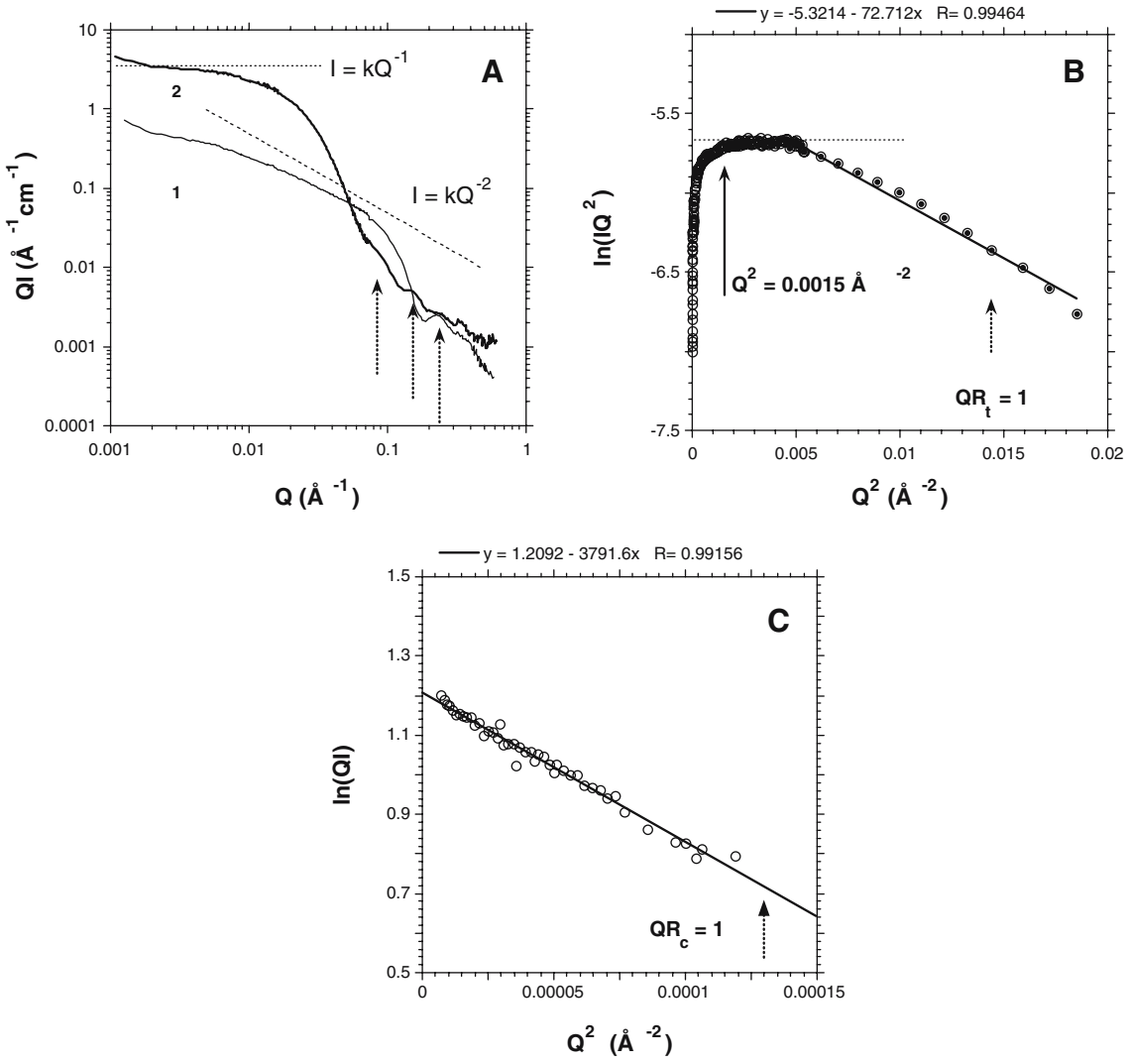

Fig. 1 SANS of DABCO-DC aqueous gels (0.5 M NaCl). **a** Cross-sectional intensity at two concentrations (*1*, C=0.0172 g cm^{-3}; *full line*; *2*, C=0.0336 g cm^{-3}, *bold line*). The *horizontal dashed line* is a guideline for the asymptotic low-Q scattering by cylindrical fibers. The *inclined dashed line* is a guideline for the asymptotic low-Q scattering by lamellas. Three *dotted vertical arrows* point at the oscillations revealing the cross-sectional monodispersity. **b** Extraction of structural parameters of the section of ribbon-like aggregates for the "dilute" gel. *1* The slope corresponds to a transverse dimension t~36.9 Å. **c** Extraction of structural parameters of the section of cylindrical-like bundles for the "concentrated" gel. The slope corresponds to a radius R=123 Å. The limit of Q validity (QR_C=1, with R_c being the cross-sectional radius of gyration) is indicated by a *dotted vertical arrow*

closely related derivative named NMM-DC (Terech et al. 2005) also forms ribbons in a system that does not form such bundles. The corresponding scattering signal for dilute gels can consequently be completely reproduced by the scattering form-factor function of ribbon-like fibers. With DABCO-DC gels, the scattering can be composite since a fraction of cylindrical bundles can be present at a given concentration and departures can be observed. An intriguing aspect of the ribbon-to-cylinder morphological evolution on a DABCO-DC concentration increase is the resulting monodispersity of the sections characterized by the three well-resolved large-Q oscillations (see Fig. 1a). This issue will be further considered in the "Discussion and conclusion" section.

The rheological properties of DABCO-DC salt-containing systems exhibit an elastic shear modulus significantly larger (G'/G''~5) than the loss modulus at all frequencies of the oscillatory applied stress (Fig. 2a). Such a signature typical of a soft viscoelastic solid confirms the gel-like consistency of the specimens that do not flow on a macroscopic scale if their test tubes are turned upside down. The viscoelastic linear domain is restricted to strains $\gamma<0.01$ and is typical of a rigid system. Beyond a critical value γ^*, corresponding to the yield stress σ^*, irreversible deformations invade the gel before the heterogeneous system flows: both G' and γ strongly diverge. Such a profile (Fig. 3) characterizes a rigid elastoplastic system. The variation of G' in the linear regime of deformations follows a power law (Fig. 4a) with an exponent of 2.0. A theoretical model (Jones and Marques 1990) used to describe the elasticity of rigid networks made up of cross-linked rigid fibers can be used to account for the experimental scaling laws. This model is limited to networks composed of elements that are energetic rather than entropic in their elasticity. Depending upon whether the cross-links are considered as frozen or freely hinged, two types of scaling are predicted. If frozen cross-links are considered, the model assumes a purely energetic network in which only bending of the fibers is allowed. In such networks, the fibers are considered to be rigid in that their spring constant is independent of the temperature. External forces applied to the network are transmitted through affine deformations down to a length scale being the distance between cross-links. A scaling law $G' \propto C^2$ is calculated for straight fibers (fractal dimension=1). A similar law would be found in a model for cellular solids formed with beams, struts, and hinges exhibiting plastic deformations out of the linear viscoelastic regime (Leon et al. 1998). Other models consider a mechanism for elasticity that is entropic in origin in networks where the fibers have thermal undulations. (MacIntosh et al. 1995) For an entangled solution, the theoretical scaling is $G' \sim C^{11/5}$, whereas for densely cross-

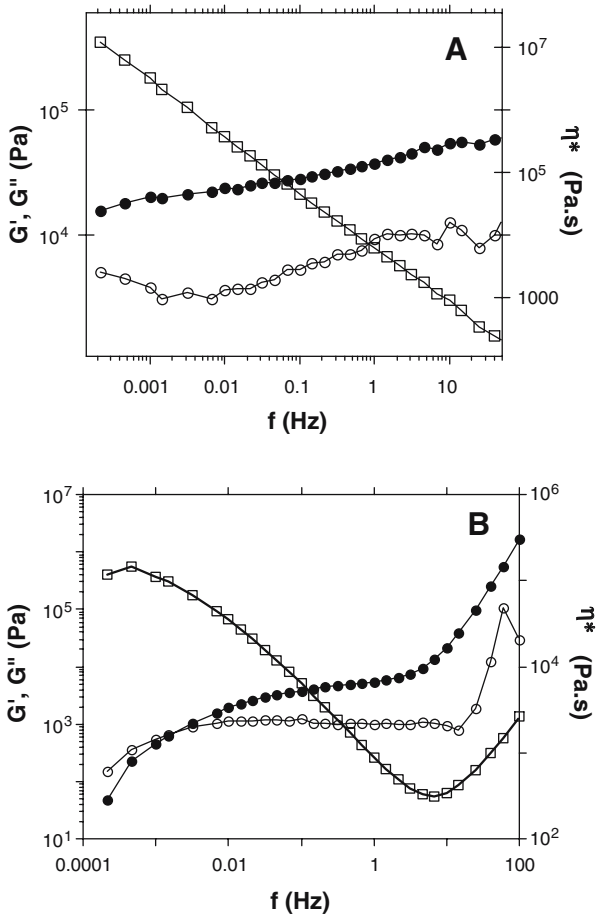

Fig. 2 Elastic shear modulus G' (•), loss modulus G'' (○), and complex viscosity η^* (□) profiles vs the frequency of an applied stress σ. **a** DABCO-DC, C=1.54 wt% (σ=5 Pa). **b** SLC, C=2.4 wt% (T_{NaOH}=0.3 M, σ=5 Pa)

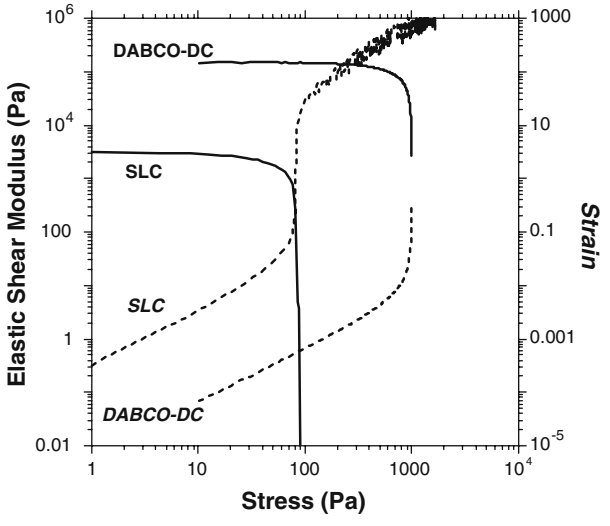

Fig. 3 Linear viscoelastic domains in an oscillatory experiment at 1 Hz frequency. DABCO-DC, C=1.5 wt% (0.5 M NaCl); SLC, C=1.2 wt%, T_{NaOH}=0.18 M. *Full lines* represent the elastic shear modulus G' and *dotted lines* the strain variation during the stress increase for the DABCO-DC and SLC system

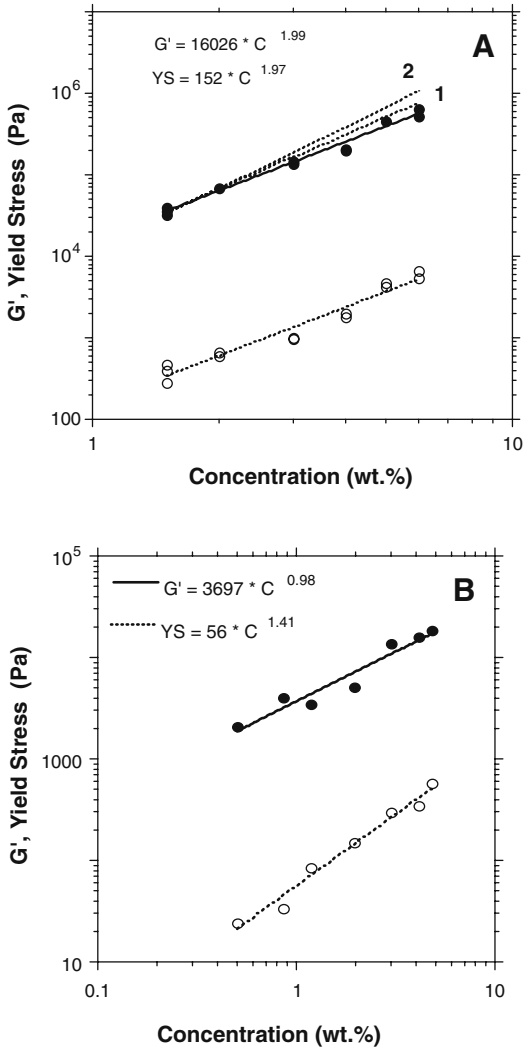

Fig. 4 G', σ^* scaling laws as a function of the concentration. Parameters used to fit power laws are indicated (exponent 2.0 for G' and yield stress). **a** DABCO-DC system. Two *dotted lines* for the scaling behavior of G' are added. *1* Exponent 2.2, *2* exponent 2.5. **b** SLC system. G' and the yield stresses have the same ordinate axis

linked gels, it is $G' \sim C^{5/2}$. Both behaviors do not provide better agreements with experiments (see Fig. 4a).

Most SAFINs in organo- or aqueous molecular gels behave as energetic networks with almost no degrees of freedom in the fiber trajectories. The absence of a significant entropic contribution is consistent with a description of the DABCO-DC network as a mesh of stiff fibers rigidly interconnected through thick cylindrical bundles produced by merging the genuine ribbons. At this stage, the exact quantity of the DABCO-DC gelator involved only in the fibers cannot be known, and thus, a more quantitative analysis cannot be done (e.g., extraction of a bending modulus). It is interesting to recall that the deformation of long fibers is easily done by bending rather than stretching/compressing, and the model for cellular solids (consistent with the present data) takes advantage of this notion. Other recent theoretical works (Head et al. 2003a,b; Levine et al. 2004; Wilhelm and Frey 2003) analyze more accurately the degree of nonaffine strain as a function of the length scale and degree of cross-links in semiflexible polymer networks. In these contexts, affine deformation would correspond to networks for which the energy is stored in the stretching modes of the fibers and a nonaffine regime where the energy is stored primarily in the bending of the fibers. Nevertheless, real SAFINs in molecular gels cannot be described as isotropic networks with punctual intersections between monodisperse filaments; their "junction zones" are not freely rotating cross-links (cross-links in SAFINs are more or less spatially extended and ordered microdomains made up of bundles of fibers), and the length polydispersity is very large. These latter conditions are the usual hypotheses of these idealized two-dimensional models that are not fulfilled with DABCO-DC gels.

The kinetic evolution of G' during the gelation process of a DABCO-DC solution is presented in Fig. 5. A sharp sigmoid profile with a characteristic time $t_{1/2}$~200 s at C=1.2 wt% stabilizes to an equilibrium value (G'_{equ}~24,000 Pa), typical of such molecular gels (Terech et al. 2000). The growth of the self-assembled ribbons and their network hinged in cylindrical "branching zones" is a fast process, which is expected for a transition from an unstable state of nonaggregated molecules (in excess with respect to the critical aggregation concentration) to a stable (or metastable) state of self-assembled ribbons (Terech and Weiss 1997). A simplified context can be that of crystallization for which Avrami (1939, 1940, 1941) developed simple equations to describe the dimensionality of the crystal

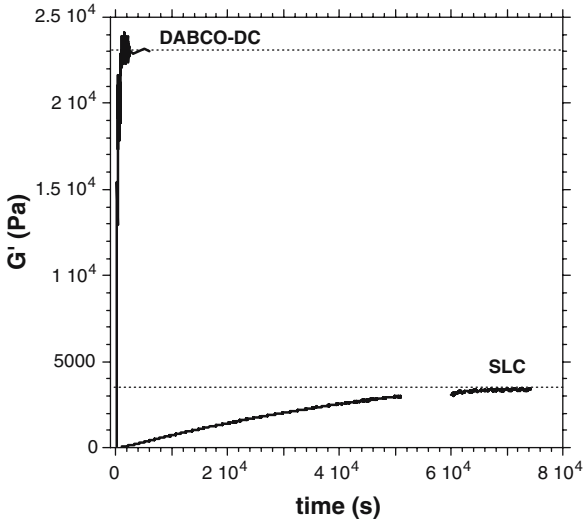

Fig. 5 Kinetic curves G' vs t during the formation of the viscoelastic systems (T=20°C). DABCO-DC, C=1.2 wt% (applied stress 1 Pa, frequency 1 Hz, NaCl=0.5 M). SLC, C=1.2 wt%, T_{NaOH}=0.18 M, applied stress 0.32 Pa, frequency 1 Hz)

growth. The modeling does not take into account the real complexity of the network elaboration in which events like branching, bundling, orderings, synergism, or collectivity between different spatial locations may occur. With DABCO-DC, the apparent exponent (not shown) in such an analytical context gives a dimensionality exponent d~0.85. The value is close enough to 1 to confirm the unidirectional character of the DABCO-DC aggregation process in the gel phases. The finding is consistent with a mechanism involving a single growth axis and a moderate anisotropy in the orthogonal plane.

Tubes (SLC system): entropic network

Small-angle X-ray and neutron-scattering experiments have shown (Terech et al. 2002) that mature suspensions of SLC at pH~12 are made up of single-walled tubes whose sections are remarkably monodisperse (external diameter D_e=520 Å, internal cylindrical cavity D_i=490 Å). Cryo-TEM measurements have also clearly demonstrated the tubular morphology and brought a range of illuminating information on the mechanism of their formation and the structural intermediates involved. Figure 6 captures, in addition to mature tubes, a step in the aggregation process showing the closing of a helical ribbon to a tube. It is interesting to note that, in contrast to DABCO-DC (or NMM-DC), the supramolecular structure of SLC ribbons is chiral (as frequently encountered with the steroid platform) and metastable. A loose helical ribbon curling in the medium is seen among tubes with very monodisperse sections. Most of the SLC tubes appear strongly oriented. This typical feature of the orientation distribution function is confirmed by cryo-TEM views or by the related anisotropic X-ray or neutron-scattering patterns (Terech et al. 2002). On the contrary, DABCO-DC gels had macroscopically random networks presenting isotropic scattering patterns when irradiated by a neutron beam at low angles of the detection (not shown). It will be shown (see "Discussion and conclusion" section) that accidental orientations in numerous domains are present on a micron scale but no resultant macroscopic ordering can be observed. Two tube ends can also be seen on the micrograph of Fig. 6. The observation is unusual in the class of SAFINs where the energy cost for end-caps is such that an infinite connectivity in the network is developing extremely fast, leaving no free ends. In particular, no stable sol phases of finite-length rods can be easily isolated in SAFINs of molecular gels (Terech and Weiss 1997). Note that those tubes are open, not capped. These two last observations already suggest that the SLC system has a much lower end-cap or, in this case, end-penalty than the DABCO-DC system and that the connectivity degree and associated interaction energy should be weaker.

The rheological curves shown in Fig. 7 support the above partial conclusion. A flattening of the shear viscosity at zero shear followed by a sharp decay with a $d\eta/d\dot{\gamma}$ slope approaching –1 is typical of semidilute solutions of rods exhibiting a solid-like behavior of complex fluids (Larson 1999). SLC suspensions at absolute rest are viscoelastic, and for instance, at a concentration C=2.4 wt%, the frequency sweep rheological signature shows (Fig. 2b) that a gel-like behavior is observed over most of the frequency scale. Nevertheless, over long timescales (small frequencies of the applied stress), liquid-like flowing properties prevail. Equilibrated gels exhibit elastic shear modulus

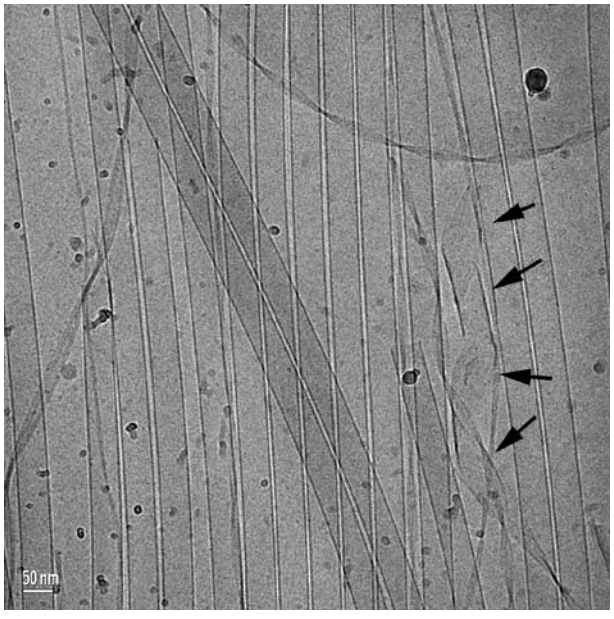

Fig. 6 Cryo-transmission electron micrograph of an SLC specimen (C=0.1 wt%) obtained during the kinetics of formation of tubes. *Black arrows* point at the wrapping process of a helical ribbon

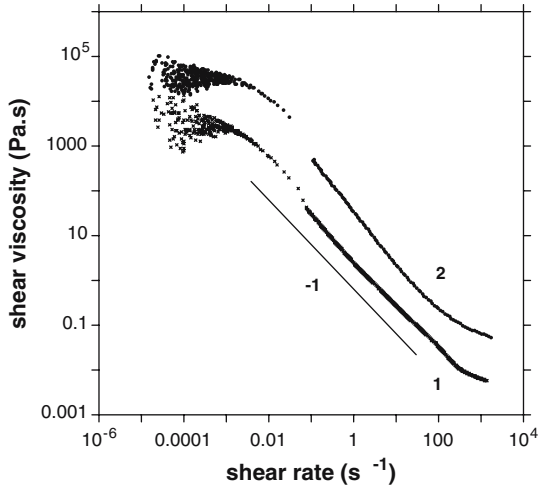

Fig. 7 Flow curves of SLC suspensions at concentrations *1*, C=0.8 wt%, *2* C=2.0 wt%. The *straight full line* is a guide for $d\eta/d\dot{\gamma}$=−1

values seven times lower (at 1 Hz) than those of the DABCO-DC system. The phenomenological pattern is consistent with weakly interacting tubes. The scaling laws of G' and the yield stress with the concentration are shown in Fig. 4b. The related exponents (≈1.0 and ≈1.4 for G' and σ^*, respectively) are much weaker than those obtained with the DABCO-DC energetic networks (2.0). These exponents have been obtained in the 0.5–5 wt% concentration range, with equilibrium values obtained in a time delay less than 10^5 s. Furthermore, the cryo-TEM view of Fig. 6 shows very rigid tubes with no flexibility (or semiflexibility), indicating that equilibrated SLC suspensions and gels are to be considered in the framework of weakly interacting rigid species. The low value of the scaling exponent indicates that entropy is gained through free rotations about the cross-link zones in the network. A refinement of the above-discussed theoretical description (Jones and Marques 1990) for rigid networks accounts for such a decreased value of the exponent. To illustrate, rigid rods freely hinged at cross-links of functionality 4 (corresponding to 1 *df* per cross-link point) show a scaling behavior with an exponent 3/2 ($G' \propto C^{3/2}$). Other systems have shown reduced scaling exponents. For instance, filamentous biopolymer networks of microtubules (Janmey et al. 1991; Xu et al. 1998) have shown a variation $G' \propto C^{1.3}$. With microtubule systems, the results were accounted for by the involvement of steric effects between the entangled polymers in networks in which the motion of the individual polymers is restricted (Ma et al. 1999). The analysis of the profile of the transition between the linear and nonlinear viscoelastic domains shown in Fig. 3 is also instructive. Compared to the DABCO-DC system, about one order of magnitude separates the yield stresses of the two systems. It emphasizes the fragility of the SLC system with respect to shear. At σ^*, the strain is strongly diverging for the DABCO-DC gel, whereas with SLC, the range of deformation available is much higher (almost 4 decades) and the onset of a second shearing regime is clearly observed. Such observations validate the option of weak interactions between tubes in an entropically driven transient network. A detailed investigation of the kinetics aspects of the network formation and equilibration as a function of concentration is under progress.

The kinetic of formation and equilibration of a tube suspension (Fig. 5) is a strikingly long process (time $t_{1/2}$~25,000 s), in particular in contrast to the DABCO-DC system at an identical concentration (C=1.2 wt%, $t_{1/2}$~200 s). The equilibrium value is also almost one order of magnitude lower (≈3,400 Pa) than DABCO-DC. Previous X-ray scattering and cryo-TEM measurements (Jean et al. 2005) have shown that although most of the basic morphological features were established at time t~100 s, variations could be observed up to t~100,000 s. A great fraction of the G' kinetics is thus assumed to be due to slow-reordering motions affecting the connectivity of the suspension. The kinetical evolution of the orientation configurations available to the SLC system is also a clear mark of an entropic network.

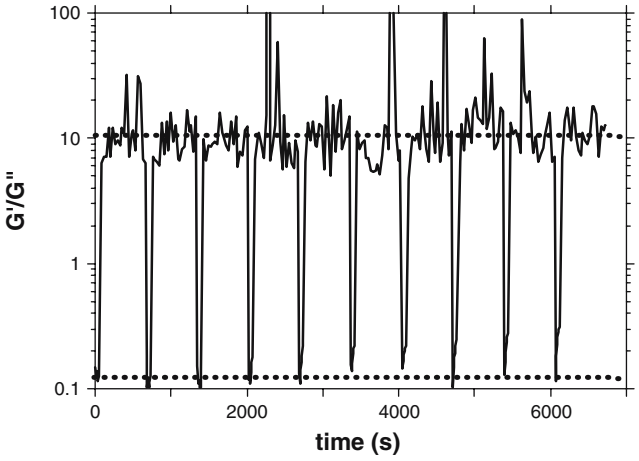

Fig. 8 "Rheological switch" composed of an SLC suspension (C=2.5 wt%, T_{NaOH}=0.25 M) submitted to an oscillatory stress of 220 Pa for 60 s, followed by 0.5 Pa for 600 s. The ratio G'/G'' varies from 10 and 0.1, i.e., gel and liquid states, following the sequence of stress pulses

A practical illustration of the shear sensitivity is shown in Fig. 8. The SLC system can instantaneously adjust under shear between the sol and gel states by an appropriate choice of applied stresses. To the sequence of stress pulses between σ=220 and 0.5 Pa, the system is successively a liquid with no significant elasticity and a gel. Such a behavior of a transient network cannot be observed with the rigidly connected DABCO-DC SAFIN.

Discussion and conclusion

The rheological properties of two systems of bile salt derivatives self-assembling in water discriminate two classes of networks. The frequency sweep profile, the scaling laws G' vs concentration, the flowing curves, and the kinetics curves provide clear evidences that the SLC system is a shear-sensitive suspension of weakly interacting self-assembled tubes. The corresponding transient network can have its orientation distribution stress-triggered in a reversible manner. The SLC SAFIN is evanescent; bundles can form accidentally or under shear. Polarized light microscopy under crossed polarizers can visualize the birefringence of such solid-like bundles. Figure 9a shows the fibrous birefringent SLC packets swimming in a less anisotropic solution. Conversely, the DABCO-DC also presents numerous small birefringent domains scattered in the immobilized network (Fig. 9b). Entropic or energetic networks can be generated using steroid hydrophobic appropriately functionalized building blocs. With SLC, the two potential connecting sites (OH and COO^-) are involved in a head-to-tail lateral aggregation reaction forming mono-

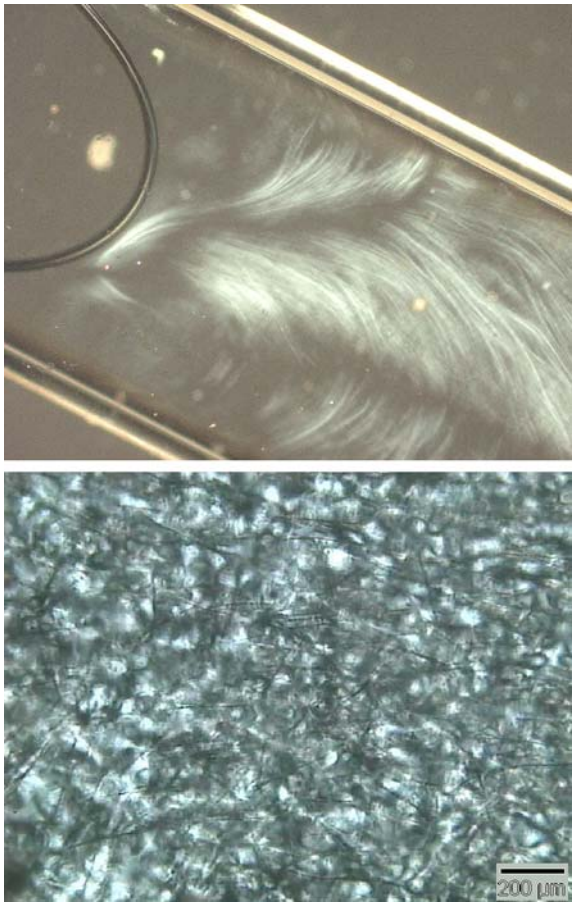

Fig. 9 Optical microscopy showing the birefringent patterns of the systems. *Top* SLC gel, C=2 wt%, T_{NaOH}=0.25 M, the width of the cell 10 mm. *Bottom* DABCO-DC gel, C=0.0336 g cm^{-3}

molecular tubular structures, with only long-range Van der Waals interactions available to optimize the connectivity. With DABCO-DC, special anisotropic crystallization proceeds in fibers with a tail-to-tail bimolecular thickness and a variable lateral extension. The positively charged bulky head group induces the hydrophobic effect, while two other connecting sites (OH) remain available for the cross-sectional extension in the ribbons and their bundles. Hydrogen bonding can participate in the connectivity of the energetic network characterized by large yield stresses and melting temperatures.

The DABCO-DC system has shown a particular sensitivity to concentration, characterized by evolution from ribbon-like structures to cylindrical ones, maintaining a high level of cross-sectional monodispersity. The feature is remarkable with respect to an ordinary bundling process, for which the dispersity is degrading, which is expected when the numbers of bundled fibers are randomly increasing. Here, with DABCO-DC, the observation suggests that statistically, a fixed number of ribbon-like fibrils is aggregated into the bundles. A similar phenomenology has also been noticed, for instance, with synthetic de novo peptide molecules (DN1), known to self-assemble into ribbon-like tapes and which can form fibers stabilized by face-to-face attraction between the tapes, having finite and monodisperse cross-sections (Aggeli et al. 1997, 2001). A theory has been proposed to account for the fiber aggregation number (Nyrkova et al. 2000). The width of the stack corresponds to an equilibrated balance between the cost of distortions of all tapes through untwisting processes and energy gain due to the face-to-face attraction of the tapes. The pertinent parameters of the theory are the cross-section of the ribbons, their intrinsic twist strength, the bend and twist elastic constants, and the energy of inter-ribbon face-to-face attraction. When the primary ribbons are not strongly twisted and the ratio of the bending modulus to the twist modulus is small enough, the region of stable fibers is wide (and is independent directly of the concentration). This situation can be also that of DABCO-DC self-assembled ribbons since large pitch values would not be probed in the experimental angular range of SANS experiments and scanning electron micrographs of the solid xerogels (dried gels) do not show clear evidences of supramolecular chirality. Eventually, four DABCO-DC ribbons (small cross-sectional axis~30 Å, large cross-sectional axis~160 Å) aggregate per cylindrical untwisted bundle (<R>~60–75 Å).

In summary, rheological properties of two classes of self-assembled steroids have been used to characterize two opposite classes of networks. Flowing, kinetics, and equilibrated properties are used to distinguish energetic networks (DABCO-DC) from entropic networks (SLC). These observations show that the force constant that prevents deformation is large for energetic networks. Coherently, the strength and timescale to modify the orientation distribution function of the SLC tubular species characterize the entropic nature of their transient network.

Acknowledgements Part of the work (DABCO-DC) was supported by the Indo-French Center for Promotion of Advanced Research (IFCPAR, project 2605-1), which is deeply thanked. Institut Laue Langevin (ILL, Grenoble, France) is acknowledged for providing access to the spectrometer and all technical support. O. Bros and I. Hassen are thanked for their help during the rheological measurements. Cryo-TEM was performed at the George and Hannah Krumholz Laboratory for Advanced Microscopy, part of the Technion Project of Complex Fluids, Microstructure and Macromolecules.

References

Aggeli A, Bell M, Boden N, Keen JN, Knowles PF, Mcleish TCB, Pitkeathly, M Radford SE (1997) Responsive gels formed by the spontaneous self-assembly of peptides into polymeric b-sheet tapes. Nature 386:259–262

Aggeli A, Nyrkova IA, Bell M, Harding R, Carrick L, Mcleish TCB, Semenov AN, Boden N (2001) Hierarchical self-assembly of chiral rod-like molecules as a model for peptide b-sheet tapes, ribbons, fibrils, and fibers. Proc Natl Acad Sci U S A 98(21):11857–11862

Avrami M (1939) Kinetics of phase change: I. J Chem Phys 7:1103–1112

Avrami M (1940) Kinetics of phase change: II. J Chem Phys 8:212–224

Avrami M (1941) Granulation phase change and microstructure. Kinetics of phase change. III. J Chem Phys 9:177–184

Bonincontro A, D'archivio AA, Galantini L, Giglio E, Punzo F (1999) On the micellar aggregates of alkali metal salts of deoxycholic acid. J Phys Chem B 103:4986–4991

Campanelli AR, De Sanctis SC, Chiessi E, D'alagni M, Giglio E Scaramuzza L (1989) Sodium glyco- and taurodeoxycholate: possible helical models for conjugated bile salt micelles. J Phys Chem 93:1536–1542

Conte G, Di Blasi R, Giglio E, Paretta A, Pavel, NV (1984) Nuclear magnetic resonance and X-ray studies on micellar aggregates of sodium deoxycholate. J Phys Chem 88:5720–5724

Esposito G, Giglio E, Pavel NV, Zanobi A (1987) Size and shape of sodium deoxycholate micellar aggregate. J Phys Chem 91:356–362

Glatter O, Kratky O (1982) Small angle x-ray scattering. Academic, London

Head DA, Levine AJ, Mackintosh FC (2003a) Deformation of cross-linked semiflexible polymer networks. Phys Rev Lett 91(10):108102–1/4

Head DA, Levine AJ, Mackintosh FC (2003b) Distinct regimes of elastic response and deformation modes of cross-linked cytoskeletal and semiflexible polymer networks. Phys Rev E 68:061907–1/15

Janmey PA, Euteneuer U, Traub P, Schliwa, M (1991) Viscoelastic properties of vimentin compared with other filamentous biopolymer networks. J Cell Biol 113(1):155–160

Jean B, Oss-Ronen L, Terech P, Talmon Y (2005) Monodisperse bile salt nanotubes in water: kinetics of formation. Adv Mater 17(16):728–731

Jones JL, Marques CM (1990) Rigid polymer network models. J Phys (Paris) 51:1113–1127

Larson RG (1999) The structure and rheology of complex fluids. Oxford University Press, New York

Leon EJ, Verma N, Zhang S, Lauffenburger DA, Kamm RD (1998) Mechanical properties of a self-assembling oligopeptide matrix. J Biomater Sci Polym Ed 9(3):297–312

Levine AJ, Head DA, Mackintosh FC (2004) The deformation field in semiflexible networks. J Phys Condens Matter 16:S2079–S2088

Lin Y-C, Kachar B, Weiss RG (1989) Novel family of gelators of organic fluids and the structure of their gels. J Am Chem Soc 111:5542–5551

Ma L, Xu J, Coulombe PA, Wirtz D (1999) Keratin filament suspensions show unique micromechanical properties. J Biol Chem 274(27):19145–19151

Macintosh FC, Käs J, Janmey PA (1995) Elasticity of semiflexible biopolymer networks. Phys Rev Lett 75(24):4425–4428

Mazer NA, Carey MC, Kwasnick RF, Benedek GB (1979) Quasielastic light scattering studies of aqueous biliary lipid systems. Size, shape, and thermodynamics of bile salt micelles. Biochemistry 18:3064–3075

McCrea JF, Angerer S (1960) Formation of helical strands by sodium deoxycholate as revealed by electron microscopy. Biochim Biophys Acta 42:355–357

Murata K, Aoki M, Susuki T, Harada T, Kawabata H, Komori T, Ohseto F, Ueda K, Shinkai S (1994) Thermal and light control of the sol–gel phase transition in cholesterol-based organic gels. Novel helical aggregation modes as detected by circular dichroism and electron microscopic observation. J Am Chem Soc 116:6664–6676

Nyrkova IA, Semenov AN, Aggeli A, Boden, N (2000) Fibril stability in solutions of twisted b-sheet peptides: a new kind of micellization in chiral systems. Eur Phys J B Cond Matter Phys 17:481–497

O'Connor CJ, Wallace RG (1985) Physicochemical behavior of bile salts. Adv Colloid Interface Sci 22:1–111

Rich A, Blow DM (1958) Formation of a helical steroid complex. Nature 46 (33):423–426

Sangeetha NM, Bhat S, Choudhury A, Maitra U, Terech P (2004) Properties of hydrogels derived from cationic analogues of bile acid: remarkably distinct flowing characteristics. J Phys Chem B 108:16056–16063

Schurtenberger P, Mazer N, Känzig W (1983) Static and dynamic light scattering studies of micellar growth and interactions in bile salt solutions. J Phys Chem 87:308–315

Talmon Y (1999) Cryogenic temperature transmission electron microscopy in the study of surfactant systems. In: Binks BP (ed) Modern characterization methods of surfactant systems. Marcel Dekker, New York, pp 147–178

Terech P, Weiss RG (1997) Low molecular mass gelators of organic liquids and the properties of their gels. Chem Rev 97 (8):3133–3159

Terech P, Pasquier D, Bordas V, Rossat C (2000) Rheological properties and structural correlations in molecular organogels. Langmuir 16:4485–4494

Terech P, De Geyer A, Struth B, Talmon Y (2002) Self-assembled monodisperse steroid nanotubes in water. Adv Mater 14(7):495–498

Terech P, Sangeetha NM, Deme B, Maitra U (2005) Self-assembled networks of ribbons in molecular hydrogels of cationic deoxycholic acid analogs. J Phys Chem B 109:12270–12276

Wilhelm J, Frey E (2003) Elasticity of stiff polymer networks. Phys Rev Lett 91 (10):108103–108104

Xu J, Palmer A, Wirtz D (1998) Rheology and microrheology of semiflexible polymer solutions: actin filament networks. Macromolecules 31:6486–6492

Zakrzewska J, Markovic V, Vucelic D, Feigin L, Dembo A, Mogilevsky L (1990) Investigation of aggregation behavior of bile salts by small-angle X-ray scattering. J Phys Chem 94: 5078–5081